The organic solute transporter α-β, Ostα-Ostβ, is essential for intestinal bile acid transport and homeostasis

Anuradha Rao*, Jamie Haywood*, Ann L. Craddock*, Martin G. Belinsky†, Gary D. Kruh‡, and Paul A. Dawson*§

*Department of Internal Medicine, Section on Gastroenterology, Wake Forest University School of Medicine, Medical Center Boulevard, Winston–Salem, NC 27157; †Medical Science Division, Fox Chase Cancer Center, Philadelphia, PA 19111; and ‡Department of Medicine, Section of Hematology/Oncology, University of Illinois, Chicago, IL 60612

Communicated by David W. Russell, University of Texas Southwestern Medical Center, Dallas, TX, December 28, 2007 (received for review November 28, 2007)

The apical sodium-dependent bile acid transporter (Asbt) is responsible for transport across the intestinal brush border membrane; however, the carrier(s) responsible for basolateral bile acid export into the portal circulation remains to be determined. Although the heteromeric organic solute transporter Ostα-Ostβ exhibits many properties predicted for a candidate intestinal basolateral bile acid transporter, the *in vivo* functions of Ostα-Ostβ have not been investigated. To determine the role of Ostα-Ostβ in intestinal bile acid absorption, the *Ostα* gene was disrupted by homologous recombination in mice. *Ost$\alpha^{-/-}$* mice were physically indistinguishable from wild-type mice. In everted gut sac experiments, transileal transport of taurocholate was reduced by >80% in *Ost$\alpha^{-/-}$* vs. wild-type mice; the residual taurocholate transport was further reduced to near-background levels in gut sacs prepared from *Ost$\alpha^{-/-}$Mrp3$^{-/-}$* mice. The bile acid pool size was significantly reduced (>65%) in *Ost$\alpha^{-/-}$* mice, but fecal bile acid excretion was not elevated. The decreased pool size in *Ost$\alpha^{-/-}$* mice resulted from reduced hepatic Cyp7a1 expression that was inversely correlated with ileal expression of fibroblast growth factor 15 (FGF15). These data indicate that Ostα-Ostβ is essential for intestinal bile acid transport in mice. Unlike a block in intestinal apical bile acid uptake, genetic ablation of basolateral bile acid export disrupts the classical homeostatic control of hepatic bile acid biosynthesis.

cholesterol | liver disease | mouse model | nuclear receptor

Bile acids are synthesized in the liver, secreted into bile, and delivered to the small intestine, where they act to facilitate absorption of fats and fat-soluble vitamins. Intestinal bile acids are efficiently absorbed by the terminal ileum and exported into the portal circulation for return to the liver and resecretion into bile (1). Many of the transporters that function to maintain the enterohepatic circulation of bile acids have been identified, including the Na-taurocholate cotransporting polypeptide (Ntcp; *Slc10a1*) and bile salt export pump (Bsep; *Abcb11*), which mediate hepatocytic uptake and export, respectively, and apical sodium-dependent bile acid transporter (Asbt) (*Slc10a2*), which mediates uptake across the apical brush border member in ileum (2). Notably absent from this list is the intestinal basolateral transporter responsible for bile acid export from enterocytes into portal blood, and this represents an important missing link in our understanding of the enterohepatic circulation. Recently, the heteromeric transporter Ostα-Ostβ was identified as a candidate ileal basolateral bile acid transporter by using a transcriptional profiling approach (3). There is abundant evidence supporting a role for Ostα-Ostβ in intestinal basolateral bile acid transport, including: (*i*) Ostα and Ostβ are highly expressed in ileum, and their expression closely parallels that of the Asbt (3, 4); (*ii*) expression of mouse Ostα-Ostβ protein, which is composed of two subunits, a 352-aa polytopic membrane protein (Ostα) and a 154-aa type I membrane protein (Ostβ) (5), is largely restricted to the lateral and basal membranes of ileal enterocytes (3); (*iii*) Ostα-Ostβ efficiently transports the major species of bile acids when expressed in transfected cells (3, 4); and (*iv*) expression of Ostα and Ostβ mRNA is positively regulated via the bile acid-activated nuclear receptor farnesoid X receptor (FXR) (6–9), thereby providing a mechanism to ensure efficient export of bile acids and protection against their cytotoxic accumulation. Although these data are consistent with a role in bile acid transport, the *in vivo* functions of Ostα-Ostβ have not been investigated. To elucidate the *in vivo* role of Ostα-Ostβ in intestinal bile acid absorption, we produced and characterized mice with a disruption in *Ostα*.

Results

Inactivation of *Ostα* in Mice. A targeting construct was designed to replace the proximal promoter and exons 1 and 2 of mouse *Ostα* with a neomycin resistance gene by homologous recombination (Fig. 1*A*). Disruption of *Ostα* was confirmed by Southern blotting [supporting information (SI) Fig. 7*B*]. In *Ost$\alpha^{-/-}$* mice, Ostα mRNA was not detected by real-time PCR (Fig. 1*B*), and full-length or alternatively spliced *Ostα* transcripts were not detected by Northern blot hybridization of intestinal RNA (SI Fig. 8*A*). As predicted from the loss of mRNA expression, Ostα protein was not detected in *Ost$\alpha^{-/-}$* mice (SI Fig. 8*B*). Because Ostα-Ostβ functions as an obligate heterodimer (3, 10), and their relative expression levels appear to be coordinately regulated (6, 7, 9, 11), expression of the Ostβ subunit was also examined. Although Ostα mRNA expression was decreased to undetectable levels, Ostβ mRNA remained highly expressed (Fig. 1*C*). We next explored whether unpartnered Ostβ protein would accumulate in *Ost$\alpha^{-/-}$* mice. Remarkably, Ostβ protein was almost undetectable in *Ost$\alpha^{-/-}$* mice (Fig. 1*D*; SI Fig. 8*B*). As quantified by densitometry, the expression of Ostβ protein was decreased by >95% in small intestine, kidney, cecum, and colon.

Phenotype of *Ost$\alpha^{-/-}$* Mice. *Ost$\alpha^{-/-}$* mice are viable and fertile; crosses between heterozygous mice produced the predicted Mendelian distribution of wild-type and mutant genotypes. *Ost$\alpha^{-/-}$* mice were indistinguishable from *Ost$\alpha^{+/-}$* or wild-type littermates in terms of survival and gross appearance, with the exception of a small growth deficit observed in *Ost$\alpha^{-/-}$* pups (SI Fig. 9). In addition, adult male *Ost$\alpha^{-/-}$* mice (3 months of age) had significantly longer small intestines than wild-type mice (male mice: *Ost$\alpha^{+/+}$*, 41.2 ± 1.3 cm vs. *Ost$\alpha^{-/-}$*, 47.7 ± 1.7 cm;

Author contributions: A.R. and P.A.D. designed research; A.R., J.H., A.L.C., and P.A.D. performed research; M.G.B. and G.D.K. contributed new reagents/analytic tools; A.R. and P.A.D. analyzed data; and A.R., G.D.K., and P.A.D. wrote the paper.

The authors declare no conflict of interest.

§To whom correspondence should be addressed. E-mail: pdawson@wfubmc.edu.

This article contains supporting information online at www.pnas.org/cgi/content/full/0712328105/DC1.

© 2008 by The National Academy of Sciences of the USA

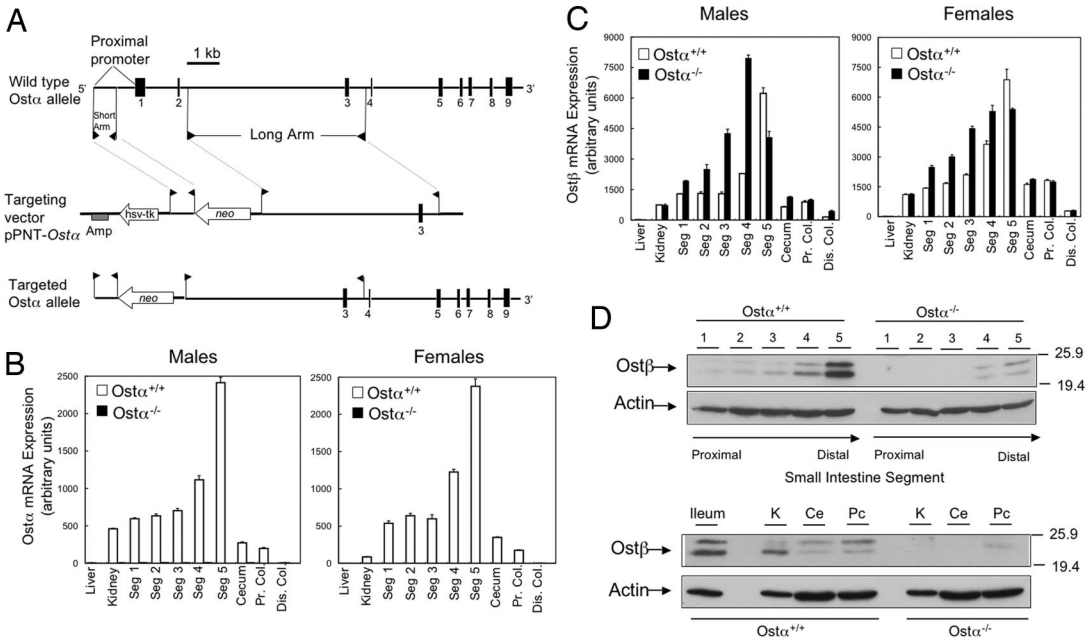

Fig. 1. Knockout of mouse *Ostα*. (*A*) Schematic showing the strategy used to delete *Ostα*. (*B*) Quantitation of *Ostα* mRNA expression (Seg 1-5, small intestinal segments 1–5; Pr. Col., proximal colon; Dis. Col., distal colon). (*C*) Quantitation of Ostβ mRNA expression. Pooled aliquots of RNA ($n = 5$) prepared from individual mice of the indicated genders and genotypes were analyzed by real-time PCR. (*D*) Analysis of Ostβ protein expression in male wild-type and $Ost\alpha^{-/-}$ mice. (*Upper*) Protein extracts were prepared from small intestinal segments of individual mice ($n = 5$), pooled, and aliquots (50 μg) were subjected to immunoblotting analysis. (*Lower*) Pooled aliquots ($n = 5$) of protein extracts from ileum (10 μg) or from kidney (*K*), cecum (Ce), and proximal colon (Pc) (50 μg) were subjected to immunoblotting analysis. The blots were probed sequentially by using antibodies to Ostβ and β-actin.

$n = 9$–11; $P = 0.0057$) (female mice: $Ost\alpha^{+/+}$, 40.3 ± 1.6 cm vs. $Ost\alpha^{-/-}$, 44.7 ± 2.0 cm; $n = 7$; $P > 0.05$), and $Ost\alpha^{-/-}$ mice exhibited small intestinal hypertrophy. This small intestinal phenotype was not observed in $Asbt^{-/-}$ or $Mrp3^{-/-}$ mice. No intestinal inflammation or diarrhea was observed in $Ost\alpha^{-/-}$ mice maintained on a chow diet. Plasma parameters were measured at 3 months of age and did not differ significantly between wild-type and $Ost\alpha^{-/-}$ mice, with the exception of lower plasma cholesterol and triglyceride levels in female $Ost\alpha^{-/-}$ mice (SI Table 1). Because the organic anion transporter Mrp3 has been proposed to participate in intestinal basolateral bile acid transport, a limited number of $Ost\alpha^{-/-}Mrp3^{-/-}$ mice were also generated. Crossing heterozygous ($Ost\alpha^{+/-}Mrp3^{+/-}$) mice produced the predicted Mendelian distribution of wild-type and mutant genotypes; $Ost\alpha^{-/-}Mrp3^{-/-}$ mice exhibit a phenotype similar to $Ost\alpha^{-/-}$ mice with regard to survival, gross appearance, and growth (data not shown).

Intestinal Bile Acid Transport. Everted gut sac preparations of Wilson and Wiseman (12) were used to investigate the contribution of Ostα-Ostβ and other transporters to intestinal bile acid transport. In agreement with previous studies using everted gut sacs (13) or *in situ* perfused small intestine (14), the mucosal-to-serosal transport of taurocholate (TC) in wild-type mice was largely restricted to distal small intestine (SI Fig. 10*A*); ileal TC transport was >20-fold higher in ileal vs. proximal segments of small intestine (Fig. 2; SI Fig. 10*A*). Hence, the contribution of transporters known or hypothesized to be involved in intestinal bile acid absorption was examined by using everted jejunal (segment 2) or ileal (segment 4) sacs prepared from the following genotypes: $Ost\alpha^{+/+}$ and $Ost\alpha^{-/-}$ littermates, $Ost\alpha^{+/+}$

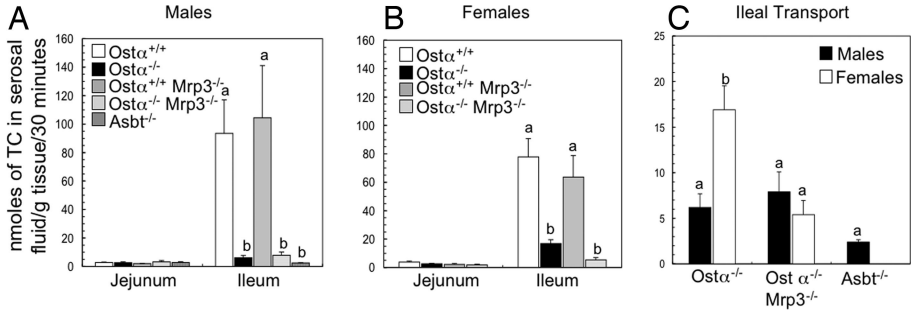

Fig. 2. Mucosal-to-serosal transport of taurocholate in mouse everted jejunal and ileal gut sacs. (*A* and *B*) Everted gut sacs were prepared from mice of the indicated genders and genotypes. The everted sacs were incubated in oxygenated KRB containing 25 μM [^{3}H]taurocholate and tracer inulin [^{14}C]carboxylic acid for 30 min at 37°C and then processed to determine the mucosal-to-serosal taurocholate transport. (*C*) Transileal taurocholate transport in $Ost\alpha^{-/-}$, $Ost\alpha^{-/-}Mrp3^{-/-}$, and $Asbt^{-/-}$ mice. Mean values ± SE are shown (males, $n = 3$–6; females, $n = 3$–7). Different letters represent significant differences between groups ($P < 0.05$). TC transport was significantly decreased in $Ost\alpha^{-/-}$ and $Ost\alpha^{-/-}Mrp3^{-/-}$ mice vs. $Ost\alpha^{+/+}$ or $Ost\alpha^{+/+}Mrp3^{-/-}$ mice (Males and Females), and in $Ost\alpha^{-/-}Mrp3^{-/-}$ vs. $Ost\alpha^{-/-}$ (Females).

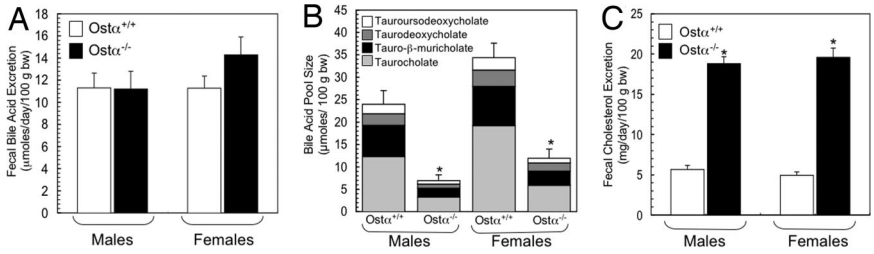

Fig. 3. Fecal lipid excretion and bile acid pool size in wild-type and *Ostα*$^{-/-}$ mice. Male and female mice (3 months of age) of the indicated genotypes were analyzed. Mean values ± SE are shown. (*A*) Fecal bile acid excretion in wild-type and *Ostα*$^{-/-}$ mice (n = 12–17). (*B*) Bile acid pool size and composition was determined by HPLC (n = 5). Bile acid pool size was significantly decreased in *Ostα*$^{-/-}$ mice (*, $P < 0.0001$). (*C*) Fecal neutral sterol excretion was measured by gas–liquid chromatography (n = 5). The *Ostα*$^{-/-}$ mice exhibited significantly increased fecal neutral sterol excretion (*, $P < 0.05$).

Mrp3$^{-/-}$ and *Ostα*$^{-/-}$*Mrp3*$^{-/-}$ littermates, and *Asbt*$^{-/-}$. For proximal jejunum, only low levels of mucosal-to-serosal TC transport were observed in gut sacs prepared from the different genotypes (2.6 ± 0.5 nmol/30 min per gram of tissue, n = 31). Compared with wild-type mice, the transileal TC transport was reduced by ≈95% and 80% in male and female *Ostα*$^{-/-}$ mice, respectively (Fig. 2). A potential explanation for the significant levels of residual transport detected in female *Ostα*$^{-/-}$ mice is that female mice express higher levels of Mrp3 (15). To test this hypothesis, gut sacs prepared from *Ostα*$^{-/-}$*Mrp3*$^{-/-}$ mice were also analyzed. Transileal transport of TC was further decreased in female but not male *Ostα*$^{-/-}$*Mrp3*$^{-/-}$ mice compared with *Ostα*$^{-/-}$ mice (Fig. 2). The residual transileal TC transport was higher than levels found in *Asbt*$^{-/-}$ mice, but the differences were not statistically significant (Fig. 2*C*). A block in basolateral bile acid export is predicted to increase the intracellular bile acid content in the everted sacs. However, the amount of tissue-associated TC in *Ostα*$^{-/-}$ and *Ostα*$^{-/-}$*Mrp3*$^{-/-}$ mice was either decreased or unchanged under these assay conditions (SI Fig. 10*B*). Efflux of TC from tissue to the serosal side (amount of TC in serosal fluid/TC associated with tissue) was decreased in *Ostα*$^{-/-}$ and *Ostα*$^{-/-}$*Mrp3*$^{-/-}$ mice (SI Fig. 10*C*).

Bile Acid Fecal Excretion and Pool Size. Decreased intestinal absorption is predicted to increase fecal bile acid excretion (16, 17). Surprisingly, however, fecal bile acid excretion, measured at 1 (SI Fig. 11) or 3 months of age (Fig. 3*A*) was similar in wild-type and *Ostα*$^{-/-}$ mice. Another hallmark of intestinal bile acid malabsorption is a decreased bile acid pool size. As shown in Fig. 3*B*, the bile acid pool was decreased by 70% and 65% in *Ostα*$^{-/-}$ male and female mice, respectively. The bile acid FTR (daily fecal bile acid excretion/pool size) was ≈0.4 pools per day in wild-type mice (males, 0.44 ± 0.08 pools per day; females, 0.43 ± 0.05 pools per day) and was elevated in *Ostα*$^{-/-}$ mice, increasing ≈5-fold in males (2.04 ± 0.47 pools per day; P = 0.01) and ≈3-fold in females (1.26 ± 0.17 pools per day; P = 0.001). Increased hepatic bile acid synthesis is a well recognized mechanism to compensate for interruption of the enterohepatic circulation of bile acids (18). In *Asbt*$^{-/-}$ mice, the bile acid pool becomes significantly enriched in TC, reflecting an increased contribution of the Cyp7a1/Cyp8b1 pathway (16). In contrast, composition of the bile acid pool is not altered in *Ostα*$^{-/-}$ mice, despite similar decreases in pool size (Fig. 3*B*). These results suggest that the normal homeostatic regulation of hepatic bile acid synthesis is altered in *Ostα*$^{-/-}$ mice. Because intestinal cholesterol absorption is particularly sensitive to variations in bile acid pool size and composition (19–21), we also examined neutral sterol excretion in *Ostα*$^{-/-}$ mice. Fecal cholesterol excretion was elevated ≈4-fold in both male and female *Ostα*$^{-/-}$ mice (Fig. 3*C*), an increase similar to that observed in *Asbt*$^{-/-}$ mice (16).

Gene Expression in Ostα$^{-/-}$ Mice. The majority of bile acids are synthesized via the Cyp7a1 pathway (20) and, as shown (16, 17), Cyp7a1 expression is increased in response to intestinal bile acid malabsorption in *Asbt*$^{-/-}$ mice (Fig. 4*A*). In contrast, Cyp7a1 mRNA expression is decreased in *Ostα*$^{-/-}$ mice. One possible mechanism for the paradoxical down-regulation of Cyp7a1 is an inappropriate induction of ileal fibroblast growth factor 15 (FGF15) expression. In distal small intestine, excess bile acids signal via FXR to induce expression of the FGF15 gene, whose protein product acts as an endocrine hormone at the liver to repress Cyp7a1 expression (22). Analysis of FGF15 mRNA expression revealed significant differences between wild-type, *Asbt*$^{-/-}$, and *Ostα*$^{-/-}$ mice. Although decreased in *Asbt*$^{-/-}$ mice (17), ileal FGF15 expression in *Ostα*$^{-/-}$ mice was elevated ≈1.8- and ≈10-fold compared with wild-type and *Asbt*$^{-/-}$ mice, respectively (Fig. 4*B*). When normalized to account for increased length and hypertrophy of the small intestine in *Ostα*$^{-/-}$ mice, total expression of FGF15 mRNA was increased ≈2-fold in segment 4 and ≈3.3-fold in segment 5, compared with wild-type mice.

To identify other potential compensatory mechanisms, the expression of intestinal genes involved in bile acid metabolism was also examined in male *Ostα*$^{-/-}$ mice (Fig. 4*C*). As also observed for Ostβ mRNA expression (Fig. 1*C*), the small intestinal gradient of expression for Asbt, Shp, and Ibabp mRNA was altered in *Ostα*$^{-/-}$ mice, with increased expression in segments 3 and 4 and reduced expression in segment 5, compared with their wild-type littermates. The expression of Mrp3 mRNA was increased in segments 2–5 in the *Ostα*$^{-/-}$ male mice.

Bile Acid Malabsorption in Cholic Acid-Fed Ostα$^{-/-}$ Mice. To bypass the altered regulation of bile acid synthesis in *Ostα*$^{-/-}$ mice, animals were fed exogenous bile acids (0.2% cholic acid diet), and feces were collected daily for 4 days to measure bile acid excretion. Wild-type and *Ostα*$^{-/-}$ mice consumed similar amounts of dietary cholic acid (≈1.0 μmol/day per gram of body weight) and maintained a constant body weight over the 4-day feeding period. The rate of fecal bile acid excretion was elevated ≈5-fold by day 2 (Fig. 5 *Inset*) and remained constant and significantly higher in *Ostα*$^{-/-}$ mice vs. wild-type mice, reflecting the block in Ostα-Ostβ-mediated transport and decreased Asbt expression. In contrast, the rate of fecal bile acid excretion in wild-type mice, although significantly lower, increased from day 2 to day 4, potentially reflecting a gradual down-regulation of Asbt expression in response to cholic acid feeding (8). As a result, cumulative fecal bile acid excretion was significantly higher in *Ostα*$^{-/-}$ compared with wild-type mice during the 4 days of bile acid feeding.

Discussion

Although many of the major plasma membrane transporters responsible for maintaining the enterohepatic circulation have

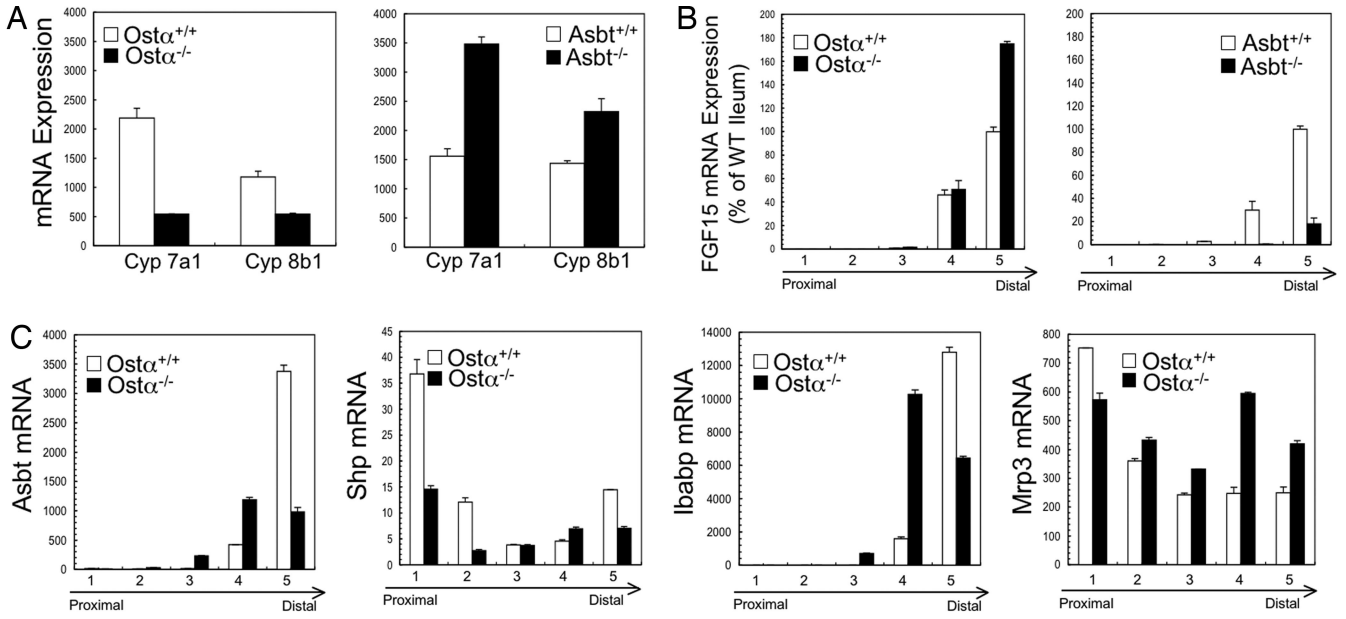

Fig. 4. Gene expression in liver and small intestine. RNA was isolated from liver and small intestinal segments of male mice from the indicated genotypes (3 months of age; C57BL/6J-129/SvEv background) ($n = 5$), pooled, and used for real-time analysis of mRNA expression. (*A*) Hepatic Cyp7a1 and Cyp8b1 mRNA expression in wild-type, *Ostα*$^{-/-}$, and *Asbt*$^{-/-}$ mice. (*B*) Small intestinal FGF15 mRNA expression in wild-type, *Ostα*$^{-/-}$, and *Asbt*$^{-/-}$ mice. FGF15 expression in distal ileum of *Ostα*$^{-/-}$ mice was elevated ≈1.8- and ≈10-fold compared with wild-type and *Asbt*$^{-/-}$ mice, respectively. (*C*) Small intestinal expression of Asbt, Shp, Ibabp, and Mrp3 mRNA in wild-type and *Ostα*$^{-/-}$ mice.

been identified over the past 20 years, the identity of the basolateral carrier(s) responsible for bile acid export from the ileal enterocyte, renal proximal tubule cells, and cholangiocyte remained uncertain. Several transporters, including Mrp3 and Ostα-Ostβ, have been proposed as candidate ileal basolateral bile acid carriers based on indirect criteria that included appropriate tissue expression, basolateral membrane localization, and ability to transport bile acids, *in vitro* (3, 23). However, subsequent studies of *Mrp3*$^{-/-}$ mice found no apparent defect in intestinal bile acid absorption (24, 25), and the *in vivo* functions of Ostα-Ostβ remained to be examined. In this study, *Ostα*$^{-/-}$ mice were generated and analyzed. *Ostα*$^{-/-}$ mice exhibited impaired transileal TC transport, a significantly reduced bile acid pool, and altered regulation of bile acid synthesis, underscoring the importance of Ostα-Ostβ for intestinal bile acid absorption and bile acid homeostasis.

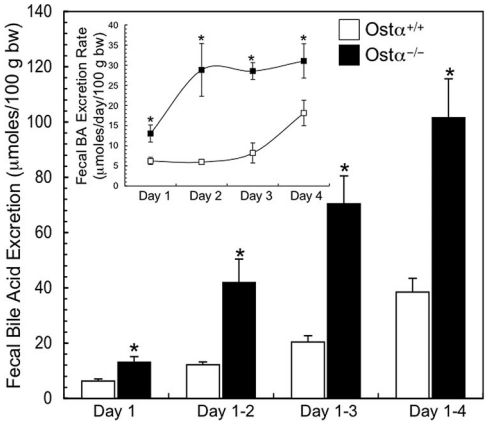

Fig. 5. Fecal bile acid excretion in male wild-type and *Ostα*$^{-/-}$ mice fed a 0.2% cholic acid-containing diet for 4 days. Feces were collected daily to measure the bile acid content and the cumulative excretion is shown (mean ± SE; $n = 6$). (*Inset*) The daily rate of fecal bile acid excretion is shown. An asterisk indicates significant differences between groups ($P < 0.05$).

By contrast with our findings in *Ostα*$^{-/-}$ mice, previous studies on *Mrp3*$^{-/-}$ mice found no significant change in transileal TC transport when measured using an Ussing chamber, and no significant changes in fecal bile acid excretion, bile acid pool size or composition, hepatic mRNA expression of Cyp7a1, or ileal mRNA expression of Ostα-Ostβ, Asbt, and Ibabp (24, 25). However, only male mice were analyzed in those studies, which express lower levels of Mrp3. Our finding that the residual TC transport in ileal gut sacs from female *Ostα*$^{-/-}$ mice was lost in *Ostα*$^{-/-}$*Mrp3*$^{-/-}$ mice suggests that Mrp3 can play a minor role in intestinal basolateral bile acid transport if expressed at sufficiently high levels.

Neither significant bile acid accumulation nor intestinal inflammation was observed in the *Ostα*$^{-/-}$ mice, suggesting the operation of compensatory protective mechanisms. Although decreased Asbt expression in distal ileum is one mechanism that limits intracellular accumulation in *Ostα*$^{-/-}$ mice (Fig. 5), the role of other efflux carriers cannot be ruled out. The small amount of residual transport observed in gut sacs and the *in vivo* results are consistent with the presence of additional unidentified minor mechanisms for intestinal basolateral bile acid efflux that, together with the reduced hepatic bile acid synthesis, would explain the finding that fecal bile acid excretion was not increased in *Ostα*$^{-/-}$ mice. Mrp4 transports bile acids and is expressed in a wide variety of tissues, including liver and small intestine (26). However, whereas Mrp4 mRNA and protein expression undergoes adaptive up-regulation in liver after cholestatic injury or bile acid feeding (27), there was no change in the intestinal expression of Mrp4 mRNA in *Ostα*$^{-/-}$ mice (data not shown). Other potential compensatory mechanisms include increased bile acid sulfation and export via the apical Mrp2 (Abcc2) or basolateral BCRP (Abcg2) carriers. However, there was no increased fecal excretion of bile acid sulfates in *Ostα*$^{-/-}$ mice (as determined by measuring fecal bile acid levels before and after solvolysis; data not shown) (28). Small intestinal

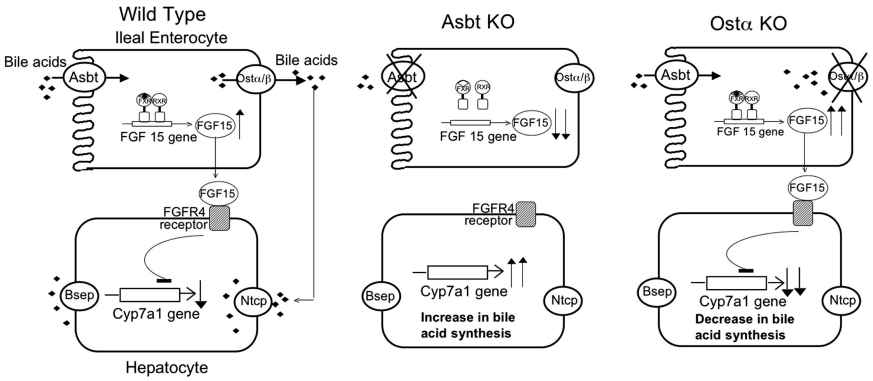

Fig. 6. Schematic model depicting the differential regulation of Cyp7a1. (Wild Type) Bile acids (♦) are absorbed from the intestinal lumen via the Asbt and activate FXR to induce FGF15 expression. Ileal-derived FGF15 acting on the liver via its receptor, FGFR4, represses Cyp7a1 expression and bile acid synthesis. (Asbt KO) A block in apical uptake of bile acids results in down-regulation of FXR target genes such as FGF15. The decreased FGF15 expression and reduced return of bile acids to the liver results in increased Cyp7a1 expression (the classical mechanism of action for bile acid sequestrants). (Ostα KO) Bile acids are taken up by the ileal enterocyte but are poorly secreted into the portal circulation. The retained bile acids activate FXR to induce FGF15 expression. Despite reduced return of bile acids to the liver, the ileal-derived FGF15 signals to repress hepatic Cyp7a1 expression and bile acid synthesis.

mRNA expression of the bile acid sulfotransferase, Sult2a1, remained extremely low and unchanged; mRNA expression of Mrp2 and BCRP was decreased in *Ost*$\alpha^{-/-}$ mice (data not shown).

In addition to establishing that Ostα-Ostβ is important for basolateral bile acid transport in the gut, another major finding of this study is that the classical feedback regulation of hepatic bile acid biosynthesis is altered in response to a block in intestinal basolateral transport. Whereas blocking apical bile acid uptake dramatically reduces ileal FGF15 expression and increases hepatic Cyp7a1 expression (17), a block in basolateral bile acid transport leads to increased FGF15 expression and reduced hepatic bile acid synthesis (Fig. 6). The decrease in hepatic bile acid synthesis in *Ost*$\alpha^{-/-}$ mice could also be due in part to decreased availability of cholesterol substrate. Fecal neutral sterol excretion is increased 4-fold in *Ost*$\alpha^{-/-}$ mice (Fig. 3*C*) and likely reflects an impaired ability of the diminished bile acid pool to promote efficient intestinal cholesterol absorption. However, arguing against this alternative hypothesis is our previous observation that hepatic bile acid synthesis is significantly increased in *Asbt*$^{-/-}$ mice, despite a similar decrease in pool size and increase in fecal neutral sterol excretion (16). Hence, these findings further support a central role of FGF15 in regulating hepatic bile acid synthesis (22), as recently demonstrated in the intestine-specific *FXR*$^{-/-}$ mice (29).

Analysis of Ostβ protein in *Ost*$\alpha^{-/-}$ mice provided insights into the consequences of dysregulated expression of the individual subunits. In addition to the loss of *Ost*α expression, Ostβ protein levels were also dramatically reduced in *Ost*$\alpha^{-/-}$ mice, despite persistently high levels of mRNA expression. This absence of Ostβ protein is consistent with previous studies, which showed that coexpression of both subunits was required for trafficking of Ostα-Ostβ from the ER to plasma membrane (3, 30). The results reported here suggest that, in the absence of assembly with Ostα, Ostβ becomes labile and is rapidly turned over, most likely by an ER-associated degradation pathway (31). Although it has been postulated that Ostβ may function as a chaperone to promote egress of other membrane proteins from the ER (10), the loss of Ostβ protein in *Ost*$\alpha^{-/-}$ mice argues that Ostβ is a dedicated partner of *Ost*α and unlikely to function as a general trafficking factor. This conclusion is also supported by a recent study in which Ost subunit expression was examined in transfected HEK293 cells and in *Ost*$\alpha^{-/-}$ mice (32).

In conclusion, our results indicate that Ostα-Ostβ is a major mechanism for intestinal basolateral bile acid transport in the mouse. Unlike blocking apical bile acid transport, blocking basolateral bile acid transport results in reduced hepatic bile acid synthesis, even in the face of a markedly reduced bile acid pool size. The results have potential significance for bile acid metabolism in humans. Whereas inhibiting Ostα-Ostβ could potentially raise plasma cholesterol levels by decreasing hepatic conversion of cholesterol to bile acids, the combination of reduced return of bile acids in the enterohepatic circulation and decreased hepatic bile acid synthesis might be exploited therapeutically to relieve the hepatic bile acid burden in some forms of cholestatic liver disease.

Materials and Methods

Animal Experiments. The Institutional Animal Care and Use Committee approved all experiments. Mice were fed ad libitum standard rodent chow or a prepared basal diet (16) containing 0.2% cholic acid. Unless indicated, the mice were fasted for ≈4 h and then killed for the experiments in this study. Serum chemistry parameters were determined at Antech Diagnostics. Plasma total cholesterol (Wako) and triglyceride (Roche Applied Science) were determined by enzymatic assay (33).

Generation of *Ost*$\alpha^{-/-}$ and *Ost*$\alpha^{-/-}$*Mrp3*$^{-/-}$ Mice. A targeting vector designed to delete the proximal promoter region and exons 1 and 2 of *Ost*α was constructed by using standard methods (16). The targeting vector was introduced by electroporation into mouse embryonic stem cells. After selection, two positive clones were identified by PCR amplification (targeting efficiency ≈1%), verified by Southern blot analysis, and clone 2C3 was injected into C57BL/6J blastocysts. High-percentage chimeric male progeny were crossed with female C57BL/6J mice (The Jackson Laboratory) to achieve germ-line transmission. For analysis of *Ost*$\alpha^{-/-}$ mice, experiments were performed with mixed-strain (C57BL/6J-129/SvEv) descendants (F_2 and subsequent generations) by using *Ost*$\alpha^{+/+}$ littermates as controls. *Ost*$\alpha^{-/-}$*Mrp3*$^{-/-}$ mice were generated by cross-breeding the corresponding null mice. The *Ost*$\alpha^{-/-}$*Mrp3*$^{-/-}$ mice are on a mixed background (C57BL/6J-129/SvEv) and were compared with *Ost*$\alpha^{+/+}$*Mrp3*$^{-/-}$ or *Ost*$\alpha^{+/+}$*Mrp3*$^{+/+}$ littermates as controls. The *Asbt*$^{-/-}$ mice used in this study are on a mixed 129/SvEv-C57BL6/J (16) or C57BL/6J background (generated by backcrossing for eight generations), as indicated.

RNA and Protein Analyses. Total RNA was extracted from frozen tissue by using TRIzol Reagent (Invitrogen). Real-time PCR analysis was performed as described (3, 8); values are means ± SD of triplicate determinations, and expression was normalized by using cyclophilin. The primer sequences used are provided (SI Table 2). Tissue extracts were prepared and subjected to immunoblotting analysis using an affinity-purified rabbit anti-mouse *Ost*α or a rabbit anti-mouse Ostβ antibody (3, 8). Antibody binding was detected by using an ECL technique (SuperSignal West Pico; Pierce). As a loading control, blots were also probed with mouse anti-β-actin antibody (Sigma).

Everted Gut Sac Transport Measurements. The small intestine was divided into four equal segments and rinsed with cold PBS, and adhering fat was removed. A 7-cm segment from each segment was weighed, gently everted, filled with Krebs Ringer Buffer (KRB), and closed using suture. The closed sacs were incubated for 30 min at 37°C in oxygenated KRB plus 25 μM [^{3}H]taurocholate (final specific activity = 55 mCi/mmol) (Perkin–Elmer) and 180,000 dpm/ml of inulin [^{14}C]carboxylic acid (2 mCi/mmol; Amersham Biosciences) (as a marker for integrity of the gut sac and for paracellular movement). A concentration of 25 μM taurocholate was selected, because this is approximately the K_m for taurocholate transport by mouse Asbt (34). After incubation, the sacs were removed, rinsed in ice-cold KRB, and weighed, and the serosal fluid was recovered. The empty sac was solubilized, and aliquots of mucosal fluid, serosal fluid, and sac tissue extract were taken to measure radioactivity. The amount of inulin [^{14}C]carboxylic acid associated with the sac or in serosal fluid after the 30-min incubation was similar for the different genders and genotypes; this value was used to correct the sac-associated [^{3}H]taurocholate for adherent fluid and to correct the serosal fluid [^{3}H]taurocholate for leakage and paracellular movement.

Fecal Bile Acid and Neutral Sterol Excretion, Bile Acid Pool Size, and Composition. Mice were individually housed in wire-bottom cages, and the feces were collected to measure the total bile acid content by enzymatic assay (16). Fecal neutral sterol content was measured by gas-liquid chromatography (35). Pool size was determined as the bile acid content of small intestine, liver, and gallbladder (24). Individual bile acid species were detected by using an evaporative light scatter detector (Alltech ELSD 800) and quantified by comparison to authentic standards purchased from Steraloids.

Statistical Analyses. Mean values ± SE are shown unless otherwise indicated. The data were evaluated for statistically significant differences by using the two-tailed Student's *t* test or by ANOVA (Tukey–Kramer honestly significant difference). Differences were considered statistically significant at $P < 0.05$.

ACKNOWLEDGMENTS. We thank Dr. Greg Shelness for critical reading of the manuscript and Dr. Ryan Temel for performing the fecal neutral sterol excretion measurements. This project was supported by National Institutes of Health Grants DK47987 (to P.A.D.) and CA73728 (to G.D.K.). A.R. is supported by a National Research Service Award (F32 DK079576).

1. Dawson PA, Shneider BL, Hofmann AF (2006) in *Physiology of the Gastrointestinal Tract*, ed Johnson LR (Elsevier Academic, Burlington, MA), pp 1437–1462.
2. Kullak-Ublick GA, Stieger B, Meier PJ (2004) Enterohepatic bile salt transporters in normal physiology and liver disease. *Gastroenterology* 126:322–342.
3. Dawson PA, *et al*. (2005) The heteromeric organic solute transporter alpha-beta, Ostαlpha-Ostβeta, is an ileal basolateral bile acid transporter. *J Biol Chem* 280:6960–6968.
4. Ballatori N, *et al.* (2005) Ostαlpha-Ostβeta: a major basolateral bile acid and steroid transporter in human intestinal, renal, and biliary epithelia. *Hepatology* 42:1270–1279.
5. Wang W, Seward DJ, Li L, Boyer JL, Ballatori N (2001) Expression cloning of two genes that together mediate organic solute and steroid transport in the liver of a marine vertebrate. *Proc Natl Acad Sci USA* 98:9431–9436.
6. Landrier JF, Eloranta JJ, Vavricka SR, Kullak-Ublick GA (2006) The nuclear receptor for bile acids FXR, transactivates human organic solute transporter-alpha and -beta genes. *Am J Physiol* 290:G476–G485.
7. Lee H, *et al*. (2006) FXR regulates organic solute transporters alpha and beta in the adrenal gland, kidney, and intestine. *J Lipid Res* 47:201–214.
8. Frankenberg T, *et al*. (2006) Regulation of the mouse organic solute transporter alpha-beta, Ostαlpha-Ostβeta, by bile acids. *Am J Physiol* 290:G912–G922.
9. Boyer JL, *et al*. (2006) Upregulation of a basolateral FXR-dependent bile acid efflux transporter Ostαlpha-Ostβeta in cholestasis in humans and rodents. *Am J Physiol* 290:G1124–G1130.
10. Seward DJ, Koh AS, Boyer JL, Ballatori N (2003) Functional complementation between a novel mammalian polygenic transport complex and an evolutionarily ancient organic solute transporter, Ostαlpha-Ostβeta. *J Biol Chem* 278:27473–27482.
11. Frankenberg T, *et al*. (2006) Regulation of the mouse organic solute transporter alpha-beta, Ostαlpha-Ostβeta, by bile acids. *Am J Physiol* 290:G912–G922.
12. Wilson TH, Wiseman G (1954) The use of sacs of everted small intestine for the study of the transference of substances from the mucosal to the serosal surface. *J Physiol* 123:116–125.
13. Lack L, Weiner IM (1961) *In vitro* absorption of bile salts by small intestine of rats and guinea pigs. *Am J Physiol* 200:313–317.
14. Lillienau J, *et al*. (1993) Negative feedback regulation of the ileal bile acid transport system in rodents. *Gastroenterology* 104:38–46.
15. Maher JM, Slitt AL, Cherrington NJ, Cheng X, Klaassen CD (2005) Tissue distribution and hepatic and renal ontogeny of the multidrug resistance-associated protein (Mrp) family in mice. *Drug Metab Dispos* 33:947–955.
16. Dawson PA, *et al.* (2003) Targeted deletion of the ileal bile acid transporter eliminates enterohepatic cycling of bile acids in mice. *J Biol Chem* 278:33920–33927.
17. Jung D, *et al*. (2007) FXR agonists and FGF15 reduce fecal bile acid excretion in a mouse model of bile acid malabsorption. *J Lipid Res* 48:2693–2700.
18. Russell DW (2003) The enzymes, regulation, and genetics of bile acid synthesis. *Annu Rev Biochem* 72:137–174.
19. Li-Hawkins J, *et al*. (2002) Cholic acid mediates negative feedback regulation of bile acid synthesis in mice. *J Clin Invest* 110:1191–1200.
20. Schwarz M, Russell DW, Dietschy JM, Turley SD (1998) Marked reduction in bile acid synthesis in cholesterol 7alpha-hydroxylase-deficient mice does not lead to diminished tissue cholesterol turnover or to hypercholesterolemia. *J Lipid Res* 39:1833–1843.
21. Shea HC, Head DD, Setchell KD, Russell DW (2007) Analysis of HSD3B7 knockout mice reveals that a 3alpha-hydroxyl stereochemistry is required for bile acid function. *Proc Natl Acad Sci USA* 104:11526–11533.
22. Inagaki T, *et al.* (2005) Fibroblast growth factor 15 functions as an enterohepatic signal to regulate bile acid homeostasis. *Cell Metab* 2:217–225.
23. Hirohashi T, Suzuki H, Takikawa H, Sugiyama Y (2000) ATP-dependent transport of bile salts by rat multidrug resistance-associated protein 3 (Mrp3). *J Biol Chem* 275:2905–2910.
24. Belinsky MG, *et al.* (2005) Analysis of the *in vivo* functions of Mrp3. *Mol Pharmacol* 68:160–168.
25. Zelcer N, *et al.* (2006) Mice lacking Mrp3 (Abcc3) have normal bile salt transport, but altered hepatic transport of endogenous glucuronides. *J Hepatol* 44:768–775.
26. Kruh GD, Belinsky MG, Gallo JM, Lee K (2007) Physiological and pharmacological functions of Mrp2, Mrp3 and Mrp4 as determined from recent studies on gene-disrupted mice. *Cancer Metastasis Rev* 26:5–14.
27. Mennone A, *et al*. (2006) Mrp4$^{-/-}$ mice have an impaired cytoprotective response in obstructive cholestasis. *Hepatology* 43:1013–1021.
28. Hirano Y, Miyazaki H, Higashidate S, Nakayama F (1987) Analysis of 3-sulfated and nonsulfated bile acids by one-step solvolysis and high performance liquid chromatography. *J Lipid Res* 28:1524–1529.
29. Kim I, *et al.* (2007) Differential regulation of bile acid homeostasis by the farnesoid X receptor in liver and intestine. *J Lipid Res* 48:2664–2672.
30. Sun AQ, *et al.* (2007) Protein–protein interactions and membrane localization of the human organic solute transporter. *Am J Physiol* 292:G1586–G1593.
31. Meusser B, Hirsch C, Jarosch E, Sommer T (2005) ERAD: the long road to destruction. *Nat Cell Biol* 7:766–772.
32. Li N, Cui Z, Fang F, Lee JY, Ballatori N (2007) Heterodimerization, trafficking and membrane topology of the two proteins, Ost alpha and Ost beta, that constitute the organic solute and steroid transporter. *Biochem J* 407:363–372.
33. Carr TP, Andresen CJ, Rudel LL (1993) Enzymatic determination of triglyceride, free cholesterol, and total cholesterol in tissue lipid extracts. *Clin Biochem* 26:39–42.
34. Saeki T, *et al*. (1999) Characterization, cDNA cloning, and functional expression of mouse ileal sodium-dependent bile acid transporter. *J Biochem (Tokyo)* 125:846–851.
35. Temel RE, *et al*. (2005) Intestinal cholesterol absorption is substantially reduced in mice deficient in both ABCA1 and ACAT2. *J Lipid Res* 46:2423–2431.